Los Alamos
NATIONAL LABORATORY
EST.1943

LA-UR-16-28498
Approved for public release; distribution is unlimited.

Title: Delta-ray Production in MCNP 6.2.0

Author(s): Anderson, Casey Alan
Mckinney, Gregg Walter
Tutt, James Robert
James, Michael R.

Intended for: 24th Conference on Application of Accelerators in Research and Industry, 2016-10-30 (Fort Worth, Texas, United States)

Issued: 2016-11-03

Disclaimer:
Los Alamos National Laboratory, an affirmative action/equal opportunity employer, is operated by the Los Alamos National Security, LLC for the National Nuclear Security Administration of the U.S. Department of Energy under contract DE-AC52-06NA25396. By approving this article, the publisher recognizes that the U.S. Government retains nonexclusive, royalty-free license to publish or reproduce the published form of this contribution, or to allow others to do so, for U.S. Government purposes. Los Alamos National Laboratory requests that the publisher identify this article as work performed under the auspices of the U.S. Department of Energy. Los Alamos National Laboratory strongly supports academic freedom and a researcher's right to publish; as an institution, however, the Laboratory does not endorse the viewpoint of a publication or guarantee its technical correctness.

Delta-ray Production in MCNP 6.2.0

C. A. Anderson,*, G. W. McKinney, J. R. Tutt, M.R. James

* *Los Alamos National Laboratory, P.O. Box 1663, Los Alamos, NM, 87545*
casey_a@lanl.gov, gwm@lanl.gov and jtutt@lanl.gov, mrjames@lanl.gov

INTRODUCTION

In an electronic inelastic collision, an energetic charged particle transfers energy to bound orbital electrons. When the energy imparted to the electron is higher than the ionization energy, a secondary electron is ejected from its orbit. The term knock-on electron or δ-ray is utilized for secondary electrons that are ejected from their orbit and additionally have sufficient kinetic energy to travel a significant distance from its point of interaction. As δ-rays can produce secondary interactions and ionizations in areas distant from the primary particle beam, they are an important feature for modeling particle physics with Monte-Carlo methods.

The all-particle, all-energy Monte-Carlo radiation transport code MCNP™ has been capable of heavy-ion and charged-particle transport following the convergence of MCNPX and MCNP5 into MCNP6[1]. Until recently, the production of secondary electrons through knock-on collisions has been limited to the transport of electrons and positrons. For the electronic stopping of heavy-ion charged particles, the energy transferred to the electron was deposited locally. In the newest release of MCNP, MCNP 6.2.0, δ-ray production has now been extended for all energetic charged particles.

This paper provides a description of this new δ-ray production (DRP) feature in MCNP 6.2.0, as well as providing results for several benchmarks and other examples demonstrating its utility.

THEORY

The DRP capability in MCNP is based off the analytical formulations described by Rossi [2] and ICRU Report 37 [3], which are briefly described here.

The total number of δ-rays produced from charged-particle interactions can be given by:

$$N_\delta = \Sigma_{in,T} \Delta x \tag{1}$$

where N_δ is the number of δ-rays produced, Δx is the step length, and $\Sigma_{in,T}$ is the total inelastic cross section for δ-ray production in a given energy range. For an incident charged particle of energy β, the inelastic cross section for an energy transfer W to an electron is given by:

$$\Sigma_{in}(\beta, W) = N_e \frac{2\pi r_e^2 m_e c^2}{\beta^2} z^2 \frac{dW}{W^2} \left[1 - \beta^2 \frac{W}{W_{max}} + K\right] \tag{2}$$

where N_e is the electron density, r_e is the electron radius, $m_e c^2$ is the electron mass energy, β^2 (v^2/c^2) is the energy of the primary particle, z is the charge of the primary particle, and W_{max} is the maximum potential kinetic energy transferred to the electron. The parameter K is a value to account for spins (s), given by:

$$K = \begin{cases} 0, & s = 0 \\ \frac{1}{2}\left(\frac{W}{E+m_e c^2}\right), & s = \frac{1}{2} \end{cases} \tag{3}$$

In order for a δ-ray to be produced, a minimum amount of energy W_{min} needs to be transferred to the electron in order to reach its ionization energy and additionally be transported a sufficient distance from the primary particle. The total inelastic cross section for δ-rays produced between this threshold energy and the maximum energy transfer becomes:

$$\Sigma_{in,T}(\beta) = \int_{W_{min}}^{W_{max}} \Sigma_{in}(\beta, W) dW \tag{4}$$

which can be explicitly solved:

$$\Sigma_{in,T}(\beta) = N_e \frac{2\pi r_e^2 m_e c^2}{\beta^2} z^2 \left[\left(\frac{1}{W_{min}} - \frac{1}{W_{max}}\right) - \beta^2 ln\left(\frac{W_{max}}{W_{min}}\right) + G\right] \tag{5}$$

where G is the spin correction given by:

$$G = \begin{cases} 0, & s = 0 \\ \frac{W_{max} - W_{min}}{E + m_e c^2}, & s = \frac{1}{2} \end{cases} \tag{6}$$

Combining equations 1 and 5, the analytical formulation for δ-ray production becomes:

$$N_\delta = N_e \frac{2\pi r_e^2 m_e c^2}{\beta^2} z^2 \left[\left(\frac{1}{W_{min}} - \frac{1}{W_{max}}\right) - \beta^2 ln\left(\frac{W_{max}}{W_{min}}\right) + G\right] \Delta x \tag{7}$$

Following conservation of momentum, a secondary electron of energy W created by a particle with mass m and velocity v is deflected at an angle ϕ given by:

$$W = 2mv^2 \cos^2 \phi \tag{8}$$

δ-ray production in MCNP

The DRP capability in MCNP, which is off by default, is activated using the 17th entry on the PHYSICS data card. Referred to as the DRP parameter, this takes the form:

```
PHYS:<pl>  16j  Wmin
```

where pl is the primary particle producing the secondary electrons and W_{min} is the threshold minimum value for δ-ray production, given in MeV. The requirements for pl is a charged particle; photons and neutrons will not work as they do not

directly produce δ-rays. The value of W_{min} can be anywhere from 1 to 1022 keV, while specifying a "−1" provides the default DRP parameter of 20 keV and setting it to "0" turns off δ-ray production.

With the addition of this value W_{min}, along with the particle and material parameters (Z, β, N_e) specified elsewhere in the MCNP input deck, the total inelastic cross-section is computed based off of Equation 5. After sampling a distance to the next inelastic scattering event (Δx), the total number of δ-rays (N_δ) produced in this range is determined from Equation 7, using a random number to provide an integer value. For each δ-ray, the source location along the step distance Δx is sampled. The kinetic energy of the electron W is sampled based off Equation 2 using a rejection sampling scheme. For an accepted energy W, the direction vector, relative to the primary particle, is determined from Equation 8. With a known source location, direction, and energy, this electron is banked for future transport.

This process is repeated until the primary charged particle falls below the threshold limit of transport, δ-ray production, or leaves the problem geometry. The total number of knock-on electrons produced from these collision is provided in the summary table in the MCNP output file.

Selection of the threshold value W_{min}

The formulations for δ-ray production provided here and implemented in MCNP are only accurate for secondary electron energies (W) greater than ≈10 keV, as more complex processes dictate their production at lower energies. Additionally, the number of secondary electrons produced exponentially increases at lower energies as seen in Equation 2, significantly increasing the computational demand for modeling and transport. Therefore, it is important to select a value of W_{min} that accurately models the true physics of secondary electron production in the system, and additionally will not negatively impact computational performance.

METHODS

To test the capability of the DRP treatment in MCNP, three separate benchmarks comparing MCNP results to previously-published results, along with three additional examples showing its usage, are provided here.

Benchmark problems

Tidman and Bradt emulsions

For the first two benchmarks, the total number of δ-rays generated in MCNP was compared to the experimental results measured in nuclear emulsions. Tidman et al. [4] measured the emulsions from energetic protons in an Ilford type G5 plate, factoring in the sensitivity of the plate to get a theoretical number of δ-rays produced in a distance within the plate. Similarly, Bradt et al. [5] measured δ-ray emulsions from cosmic α-particles and protons using an Eastman type NTB plate and Ilford C2 plate, respectively. To eliminate the production of knock-on electrons from secondary interactions, including other δ-rays, other secondary interactions were eliminated in MCNP by setting the 8^{th} entry on the LCA card to "−2". With this card activated, the total number of δ-rays simulated in the emulsion material can be quantified and compared to these measured results.

FLUKA and experimental TEPC data

For the last benchmark example, MCNP results were compared to FLUKA and experimental measurements provided by Northum et al. [6]. In this example, a fully-ionized 360 MeV/nucleon iron beam was incident upon on a tissue-equivalent proportional counter (TEPC). The TEPC is designed to simulate a 1 μm region of human tissue using a cylinder of low-density propane surrounded by a wall of A-150 plastic. Energy deposited from secondary electrons and total lineal dose (secondary electrons and 360 MeV/nucleon iron beam) in the propane center was compared in MCNP to the results from this report.

Additional examples

Thin-film YBCO superconductor

In the first example problem, simulations for the total energy deposited within a thin-film (100 nm thick) YBCO superconductor are performed, as energy deposited from ions can significantly impact the functionality of the material. To see how the DRP feature can alter results, the total energy deposited is compared with different DRP cutoff values using an +F6 tally. In previous versions of MCNP, and additionally when the DRP treatment is turned off, all energy transferred from the primary charged-particle is deposited locally. While this may remain a reasonable assumption for most applications due to the low-range of secondary electrons, thin-films would allow a significant number of low-energy electrons to escape the material. Consequently, it is expected using the DRP capability with low threshold values will decrease the total accumulated dose in the thin film.

Incident muon on SNM

In the last example, we look at the photon signatures generated from a 100 MeV negative muon (μ^-) beam incident on spent nuclear material (SNM). For this example, uranium-238 was used to simplify the material properties of SNM. Two separate scenarios were tested; one where the muons fully pass through the uranium (1 cm thick), and another where the muons are fully stopped (4 cm thick). When the negative muons are stopped in the uranium, muonic x-rays and nuclear fissions are produced from muonic interactions with the uranium nucleus. The high-energy photons produced from these reactions and the secondary interactions should dominate the total photon signatures generated on the uranium target, creating minor changes when DRP is activated. For the cases where the muons fully pass through the material, the majority of the photons are generated from interactions with the secondary electrons. As such, significant differences are expected to be observed with the DRP capability for the 1 cm example. The total photon signatures within the sphere (using an F4 tally) are compared with and without the DRP treatment using a 50 keV cutoff.

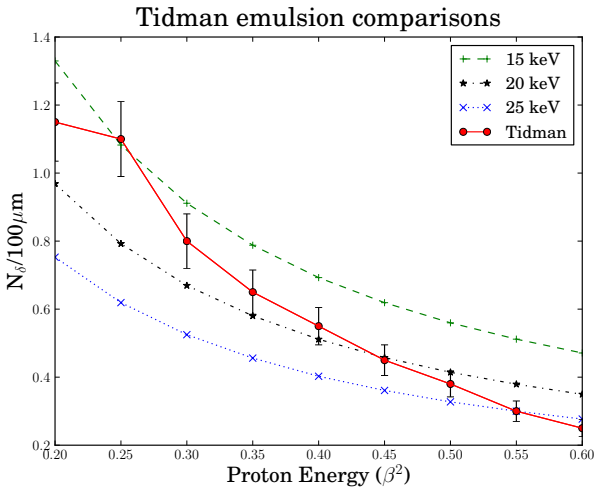

Fig. 1: Tidman results compared to MCNP results with different cutoff values

RESULTS

Benchmarks

Tidman and Bradt emulsions

The results in Figure 1 show a comparison of the measured emulsion data from Tidman (red) with the MCNP results for different cutoff values. For the cutoff values around the estimated minimum value of the Tidman paper (20 keV), good agreement is observed.

A comparison of the δ-rays produced in MCNP from cosmic α and proton sources are found in Table I. To accurately compare the results, the data taken from Bradt included corrections for their estimated δ-ray counting efficiency, which were 16% for the Eastman NTB plate and 10% for the Ilford C2 plate. In addition, only δ-rays between 10 and 30 keV are counted in their results. For the MCNP results, two separate runs with DRP parameters of 10 keV and 30 keV were modeled, and their difference reported. For different proton and α energies and different emulsion plates, good agreement is seen between MCNP and the results from Bradt.

Energy (MeV)	**Emulsion Plate**	$N_\delta/100\mu m$ **(Bradt)**	$N_\delta/100\mu m$ **(MCNP)**
368 (α)	NTB	4.75	2.94
168 (α)	NTB	8.13	8.89
60 (proton)	Ilford	25.0	36.8

TABLE I: Emulsion results comparison of Bradt to MCNP

FLUKA and experimental TEPC data

The results of the secondary electron energy deposition and total energy deposition in the propane center of the TEPC is shown in Figure 2. Good agreement is observed between MCNP, FLUKA, and the experimental results for the total energy deposited in the TEPC center. When the DRP utility is activated, energetic electrons can carry energy outside the propane volume, lowering the total dose and providing better agreement with the measured data.

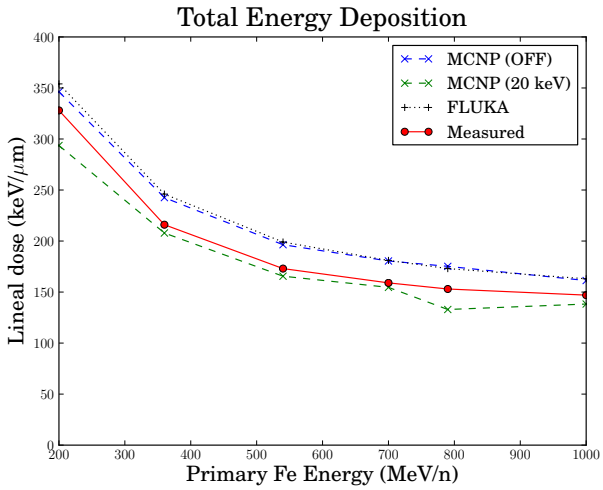

Fig. 2: Total Energy deposition in the TEPC propane center compared to experimental and FLUKA results from Northum et. al

Additional examples

Thin-film YBCO superconductor

The results of thin film energy deposition for different cutoff values are provided in Table II. For this particular example, low-energy electrons with a very low range can be transported out of the thin-film, and consequently do not deposit their energy locally in the film. As such, modeling these low-energy δ-rays using the DRP treatment significant changes the total dose within the film. With the DRP treatment turned off, or for cases of high DRP cutoff values, the energy transferred from the primary particle below this cutoff is deposited at the site of interaction, eliminating the potential for transport outside the target volume.

$\mathbf{W_{min}}$ **(keV)**	1	20	50	100	200	OFF
Energy (keV)	0.47	0.50	0.53	0.57	0.60	0.60
% Difference	22%	16%	11%	4%	0%	—

TABLE II: Energy deposited in a thin film YBCO superconductor for different DRP cutoff values

Muon SNM example

The results of the total electron and photon signatures within the uranium sphere following simulations with 100000 histories is provided in Table III. For the photon production, *br* is for brehmstrahhlung, *cap* is for electron capture, *pp* is for pair production, and *tot* is the total amount. For the electrons, *ko* refers to electrons generated from knock-on

interactions, both of the primary charged particle and other secondary particles. When the muons are stopped for the 40mm sphere, the cascade of secondary interactions in addition to δ-rays produce a significant amount of photons and electrons through a variety of means, including high-energy muonic x-rays. In contrast, the muons passing fully through the 10mm sphere produce very few secondary interactions other than δ-ray production. As a result, activating the DRP treatment will significnatly increase photon and electron production in this example.

The internal photon energy distribution within the uranium sphere with (red) and without (blue) δ-ray production is shown in Figure 3. For the 40 mm example, there are minimal differences in the photon energy distribution at high energies, as shown with nearly identical muonic X-ray signatures. When the DRP utility is activated, more low energy photons are produced due to increased electrons producing brehmstrahhlung and electron capture photons. For the 10mm example, however, significant differences in low and mid-energy photons are seen when the DRP treatment is activated, as it is the primary source of the electrons that produce photons. While not as strong or penetrating as the high energy muonic X-rays, these secondary photons are detectable on the surface and outside the sphere. Consequently, the utilization of DRP is needed in order to accurately reflect the target signatures of this muon beam.

		10mm		40mm	
DRP		**50 keV**	**OFF**	**50 keV**	**OFF**
γ	br	1.3e5	3.7e1	4.0e6	1.8 e6
	cap	9.4e4	4.3e1	6.9e6	4.4e6
	pp	0.0	0.0	9.7e4	9.7e4
	tot	1.7e5	4.9e1	7.1e6	4.6e6
e-	ko	1.1 e7	1.9e4	3.2e8	1.2e8
	tot	1.1 e7	2.0e4	3.3e8	1.2e8

TABLE III: Photon and electron signatures in the uranium sphere. Production methods are: *br* brehmstrahhlung, *cap* electron capture, *pp* pair production, *ko* knock-on, and *tot* total

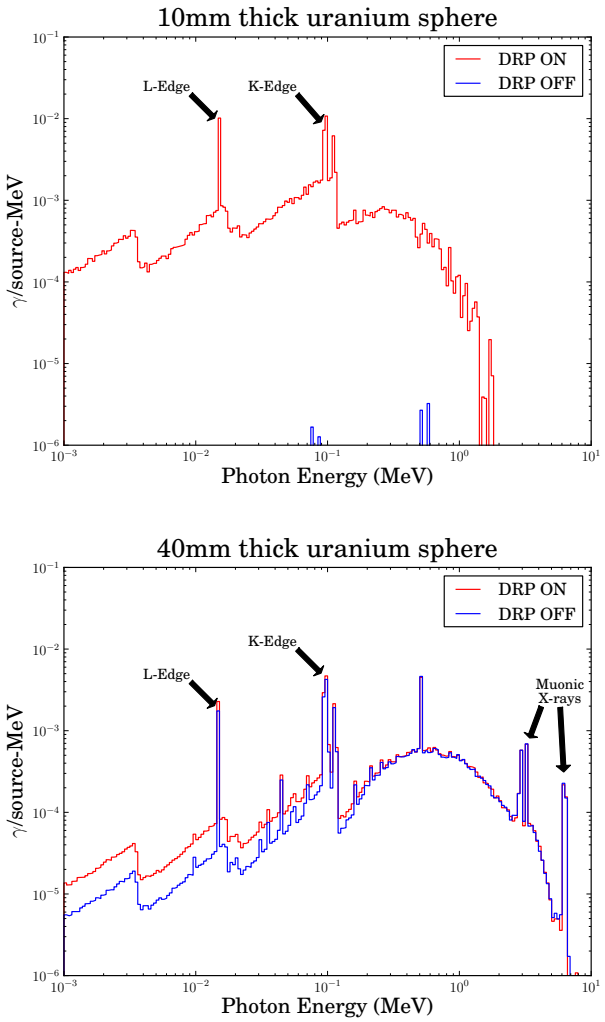

Fig. 3: Internal photon energy distributions for 100 MeV muons passing through 10 mm (top) and 40 mm (bottom) thick uranium targets

CONCLUSIONS

Good agreement for the production of δ-rays is observed when compared against other simulation codes and previously published results. In addition, we have provided several example problems that demonstrate important capabilities and considerations with the DRP treatment. As demonstrated in the thin film and muon beam examples, the selection of the DRP parameter W_{min} can significantly alter the target tally results. Convserely, the photon signatures seen in the 40mm uranium sphere muon example provides a case where the DRP treatment can likely be ignored, as the photon signature is dominated by the high-energy photons produced from other nuclear interactions. The comparatively low-energies of the photons produced from secondary δ-rays will have very minimal effect on photons leaving the SNM.

In this report, we have thoroughly tested the new δ-ray production capability for energetic charged-particles in MCNP 6.2.0.

APPENDIX

```
Simple example of activating DRP in MCNP
c Cell Cards
1  100  -1.0     -10  imp:e=1    $ inside sphere
2  0               10  imp:e=0    $ void

c Surface Cards
10 so         1.0       $ 1 cm sphere

c Data Cards
mode h e
sdef  par=h  erg=100
phys:h  16j  -1          $ DRP on, 20 keV
m100   1001 2  8016 1   $ Water
```

ACKNOWLEDGMENTS

This work has been supported by the U.S. Department of Homeland Security, Domestic Nuclear Detection Office, under competitively awarded contract/IAA HSHQDC-12-X-00251. This support does not constitute an express or implied endorsement on the part of the Government.

REFERENCES

1. D. PELOWITZ, A. FALLGREN, and G. MCMATH, "MCNP6 User's Manual, Version 6.1.1beta," *LANL report LA-CP-14-00745* (2014).
2. B. ROSSI, *High-energy particles*, Prentice-Hall, 1st ed. (1952).
3. ICRU, "ICRU Report 37: Stopping powers for electrons and positrons," (1984).
4. D. TIDMAN, E. GEORGE, and A. HERZ, "The production of delta-rays in nuclear-research emulsions," *Proc. Phys. Soc. Lond*, **66**, *A*, 1019 (1952).
5. H. BRADT and B. PETERS, "Investigation of the primary cosmic radiation with nuclear photographic emulsions," *Physical Review*, **74**, *12*, 1828–1837 (1952).
6. H. NORTHUM, S. GUETERSLOH, and L. BRABY, "FLUKA capabilities for microdosimetric analysis," *Radiation Research*, **177**, *1*, 117–123 (2012).